MTR 00B0000015

MITRE TECHNICAL REPORT

Comparison of Narrowband Adaptive Filter Technologies for GPS

March 2000

R. Rifkin
J. J. Vaccaro

Sponsor: ESC
Dept. No.: D730
Contract No.: F19628-99-C-0001
Project No.: 03006132AJ

MITRE
Center for Air Force C2 Systems
Bedford, Massachusetts

Report Documentation Page

Form Approved
OMB No. 0704-0188

1. REPORT DATE	2. REPORT TYPE	3. DATES COVERED
MAR 2000		**00-03-2000 to 00-03-2000**

4. TITLE AND SUBTITLE	5a. CONTRACT NUMBER
Comparison of Narrowband Adaptive Filter Technologies for GPS	5b. GRANT NUMBER
	5c. PROGRAM ELEMENT NUMBER
6. AUTHOR(S)	5d. PROJECT NUMBER
	5e. TASK NUMBER
	5f. WORK UNIT NUMBER
7. PERFORMING ORGANIZATION NAME(S) AND ADDRESS(ES) **MITRE Corporation,202 Burlington Road,Bedford,MA,01730-1420**	8. PERFORMING ORGANIZATION REPORT NUMBER
9. SPONSORING/MONITORING AGENCY NAME(S) AND ADDRESS(ES)	10. SPONSOR/MONITOR'S ACRONYM(S)
	11. SPONSOR/MONITOR'S REPORT NUMBER(S)

12. DISTRIBUTION/AVAILABILITY STATEMENT
Approved for public release; distribution unlimited

13. SUPPLEMENTARY NOTES

14. ABSTRACT

15. SUBJECT TERMS

16. SECURITY CLASSIFICATION OF:			17. LIMITATION OF ABSTRACT	18. NUMBER OF PAGES	19a. NAME OF RESPONSIBLE PERSON
a. REPORT	b. ABSTRACT	c. THIS PAGE			
unclassified	**unclassified**	**unclassified**		**26**	

Standard Form 298 (Rev. 8-98)
Prescribed by ANSI Std Z39-18

MITRE Department Approval:

R. T. Williams

MITRE Project Approval:

T. M. Hopkinson

Abstract

Narrowband interference can seriously degrade the performance of GPS systems. Several techniques exist for reducing this interference, including adaptive transversal filters, overlapped FFTs, and filter banks. All these techniques attempt to filter out the interference before the GPS receiver performs correlation. This paper compares these three interference suppression techniques for application to GPS. Likely VLSI-based designs with various levels of complexity (i.e., operation counts) for each technique are proposed and described. The effects of these designs as pre-processors on GPS ranging performance is then compared using computer simulation.

Acknowledgments

The authors would like to acknowledge useful conversations with Paul T. Capozza, Walter S. Kuklinski, and Daniel Moulin.

Table of Contents

List of Figures

List of Tables

Section 1

Introduction

Narrowband interference can substantially degrade the performance of the global positioning system (GPS). While the GPS signal has inherent resistance to such interference through its processing gain, in certain scenarios the gain is inadequate and additional remedies must be sought against this problem. Statistical detection theory suggests that both acquisition [1] and tracking [2] performance for GPS can be optimized in non-white noise by including as part of the matched filter a pre-filter whose spectrum is approximately the inverse of the noise plus interference power spectrum. Spectral regions containing interference are then essentially discarded by this pre-filtering.

A class of well-known techniques uses pre-filtering before correlation to sharply reduce the interference power out of the filter while having little effect on the desired GPS signal. The filter can be formed in the time domain using an adaptive transversal filter (ATF) (e.g., [3]), or in the frequency domain using overlapped fast Fourier transform (OFFT) techniques [4]. A variant of the latter technique, the filter bank (FB) [5,6] uses filtering in conjunction with the FFT to achieve better frequency resolution than the former.

This paper compares the performance of these three classes of narrowband frequency suppression strategies for application to GPS. The next section describes likely configurations for these techniques and a computer simulation developed to examine how the GPS receiver performs with these techniques in various interference environments. Section 3 discusses simulation results and Section 4 summarizes the key conclusions of this study.

Section 2

Model

This section describes the three classes of narrowband interference suppression techniques and how they are incorporated into a computer simulation for evaluating their performance when combined with GPS. All three techniques form filters for reducing the interference energy; the filter response, however, differs for each technique. Both FFT-based techniques rely on a separate threshold to decide which frequency sample values are set to zero.

2.1 Overlapped FFT-Based

As shown in Figure 1, OFFT interference suppression uses two weighted FFTs operating in parallel. For each forward FFT, the n^{th} output sample for each block of N samples, $X(n),\ n = 0,1,\ldots,N-1$, is given by:

$$X(n) = \sum_{k=0}^{N-1} w(k)\, r(k)\, e^{-2\pi i k n/N}, \tag{1}$$

where $w(k)$ and $r(k)$, $k = 0,1,\ldots,N-1$, are the weights and input signal samples, respectively. The frequency resolution for excision depends on both the sampling rate and N. Frequency excision is accomplished by comparing the magnitude of each frequency bin to a threshold and discarding (i.e., setting to zero) those bins above the threshold. Bins whose values are below the threshold remain unchanged. Several algorithms can be used to obtain a threshold [4]; here, it is set at 4 times the median absolute value of all the frequency cells. This threshold is approximately proportional to the mean noise power without interference and is set to reduce the interference power as much as possible while minimizing GPS signal degradation. Windowing helps by reducing the inherent frequency broadening of each interferer caused by the finite duration of the FFT. Fewer frequency samples are excised when windowing is performed. The second FFT and suppression algorithm running

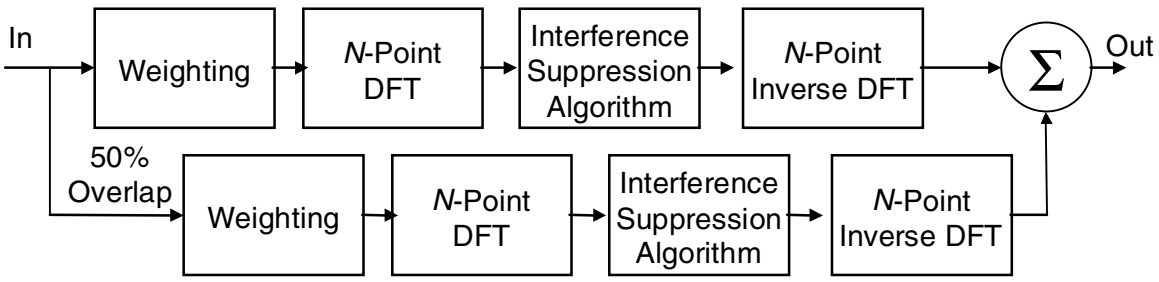

Figure 1. Overlapped FFT Design

with 50% overlap at the inverse FFT output helps to reduce (but not eliminate) the weighting loss. For the Blackman-Harris weighting examined here the loss is reduced to approximately 0.6 dB using this overlap.

2.2 Filter Bank Interference Suppression

Filter bank (FB) interference suppression represents an extension of OFFT that attempts to further reduce the weighting loss by extending the effective FFT length. The conventional FFT may be thought of as a set of N mixers at frequencies $k = 0,1,2,\ldots,N-1$ followed by lowpass filters of length N. Each FFT output bin is sampled every N samples. The FB extends this notion by allowing the spectrum estimation to occur more or less frequently and the filtering to assume arbitrary length. Typically, the spectrum estimation still occurs every N samples and the filtering extends over an integer multiple of the FFT length.

Consider the FB interference suppression design shown in Figure 2. As with the OFFT design, it consists of a conversion to a frequency representation, suppression and then a conversion back to a time representation. The initial conversion to frequency comprises three components: decimation, filtering and an FFT. The decimation lowers the sample rate into each (polyphase) filter by the FFT length N. Each polyphase filter is of length I, making the effective length of the filter bank filter NI. The design of this latter filter is described shortly. After interference suppression the inverse FFT is computed, followed by polyphase filtering and a sampling rate increase of N.

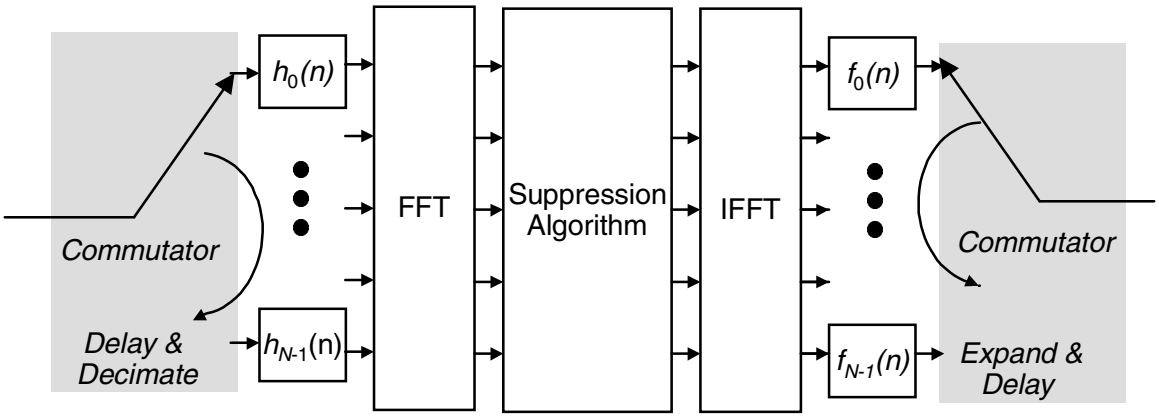

Figure 2. Filter Bank Design

The two sets of polyphase filters $\left(h_0(m), h_1(m), \ldots, h_{N-1}(m)\right)$ and $\left(f_0(m), f_1(m), \ldots, f_{N-1}(m)\right)$ are obtained similarly and designed as follows. Each polyphase filter is a decimated version of a "parent" analysis filter $h(m)$ and synthesis filter $f(m)$, respectively. Additionally, the analysis polyphase filters are time-reversed.

Assume for simplicity that the synthesis filter's frequency response is the complex conjugate of that of the analysis filter. Additionally, in a practical lowpass filter the 3 dB bandwidth is set to approximately 1/*N* and beyond a bandwidth of 2/*N* there is negligible response. Thus, only the interaction between adjacent filter bins need be considered, and the parent filters must then satisfy [5, p. 331]

$$\left|F\left(e^{2\pi i f}\right)\right|^2 + \left|F\left(e^{2\pi i (f-1/N)}\right)\right|^2 \cong 1$$

$$F\left(e^{2\pi i f}\right)F^*\left(e^{2\pi i (f-1/N)}\right) + F\left(e^{2\pi i (f-1/N)}\right)F^*\left(e^{2\pi i (f-2/N)}\right) \cong 0, \qquad (2)$$

$$0 \le f \le \frac{1}{N}$$

where upper case denotes the Fourier transform. The first equation above states the magnitude-squared response of the shifted lowpass filters sum approximately to unity between adjacent bins. At the bin edge each filter should contribute ½ to the power

response. This equation can be satisfied reasonably accurately with typical lowpass filter designs. The design adopted here uses Kaiser weighting with $I = 4$ and $N = 128$. The magnitude-square response exhibits a peak-to-peak fluctuation of less than 0.06 dB.

2.3 Adaptive Transversal Filter

Performance comparisons are based on a steady-state $2M+1$ tap linear phase ATF derived via direct matrix inversion. This ignores transient effects present in a gradient-based implementation and, therefore, represents an optimistic prediction of ATF performance. A $2M + 1$ tap linear-phase filter is developed by utilizing the M taps on each side of the center tap as a $2M$ tap linear predictor of the value at the center tap. This structure is depicted in Figure 3, where at time n the tap samples are given by $x_n, x_{n-1}, \ldots, x_{n-2M}$ and the output is

$$\begin{aligned} r_n = x_{n-M} &- x_n w_0 - x_{n-1} w_1 - \cdots \\ &- x_{n-(M-1)} w_{M-1} - x_{n-(M+1)} w_M - \cdots - x_{n-2M} w_{2M-1} \end{aligned} . \tag{3}$$

This can be re-expressed in vector notation as

$$r_n = x_{n-M} - \mathbf{w}^{\mathrm{T}} \mathbf{x}_n \tag{4}$$

where $\mathbf{w}$ is the length $2M$ vector of weights and $\mathbf{x}_n$ is the length $2M$ vector of inputs existing at time n (center sample omitted). Minimization of the output power yields the conjugated optimum weights as:

$$\mathbf{w}^* = \mathbf{R}^{-1} \rho \tag{5}$$

where ρ is the $2M \times 1$ deterministic cross-correlation vector between the center tap input and the remaining (punctured) tap inputs and $\mathbf{R}$ is the deterministic $2M \times 2M$ autocorrelation matrix of the punctured tap inputs [7].

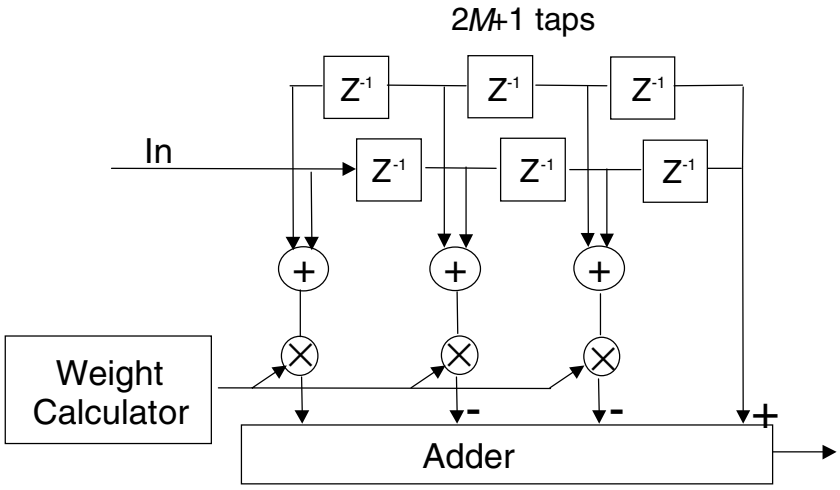

Figure 3. Adaptive Transversal Filter

Since the receiver matched filter is assumed to incorporate the anti-aliasing filter used in the receiver front end, the ATF should not attempt to correct for this filter (i.e., whiten the input samples). That is, with no narrowband interference the ATF response should be a delta function. The $2M$ degrees-of-freedom represented by the taps should not be wasted on the anti-aliasing filter. To force the Wiener solution given by (5) to ignore this filter, the data samples used to compute $\mathbf{R}$ and ρ must be preprocessed by the inverse of the anti-aliasing filter. In principle this can be accomplished by designing an FIR inverse filter. In practice, this is almost impossible because of the FIR's finite length. Moreover, it is computationally expensive. A simpler technique is to add white noise to the input samples used to compute $\mathbf{R}$ and ρ, in effect masking the effects of the anti-aliasing filter. In the simulation to be discussed, $\mathbf{R}$ is simply diagonally loaded with an additional noise power equal to the system noise level. This diagonal loading only effects the determination of the optimum weights; time-of-arrival estimation is based upon processing the original data.

2.4 Complexity Comparison

Computational complexity of the ATF is based on the simplified architectural description presented in Figure 3. With symmetric coefficients a $2M+1$ tap linear phase filter is realized with M complex multipliers and $2M$ complex adders. Complex multiplies are modeled as 6 operations (ops) and complex adders are modeled as 2 ops. Ignoring the weight calculation, the total number of ops to yield a single ATF output is

$$10\,M\ \frac{\text{ops}}{\text{output}}$$

OFFT computations based on a length-N FFT are depicted in Figure 4, where a single leg yields $N/2$ output samples.

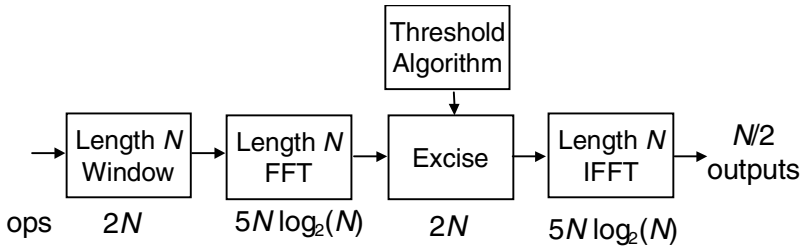

Figure 4. OFFT Complexity Model

The window is assumed to be real, each FFT butterfly has 10 ops, and the excision is a single gating of the real and imaginary values. The ops-per-output is:

$$20\log_2(N)+8\ \frac{\text{ops}}{\text{output}}.$$

Finally, the filter bank computation model is shown in Figure 5. The FFT length is designated K, to distinguish it from that used in the OFFT. The analysis and synthesis filters are real. The number of operations per output sample for the filter bank is

$$10\log_2(K) + 4I + 2 \frac{\text{ops}}{\text{output}}.$$

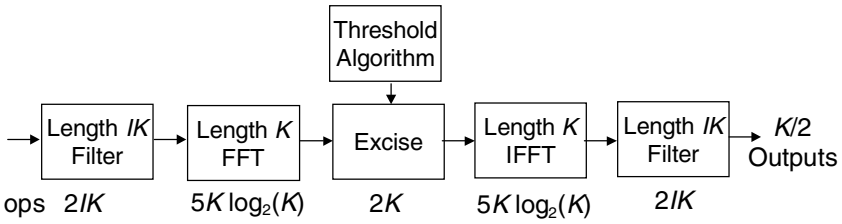

Figure 5. Filter Bank Complexity Model

As shown in the next section, the required FFT length for OFFT processing depends on both the expected number of interferers and the fraction of FFT cells that can be discarded based on performance requirements. These considerations lead to a baseline system using a length-256 FFT. A 40-tap ATF has an approximately equal computational complexity to that of a 256-pt OFFT, and is used in the simulations to establish the relative performance of these two techniques. To compare the FB with OFFT, set the FB FFT length to be proportional to the OFFT filter length ($K = cN$). The ratio of computations from OFFT to FB is

$$\frac{\text{OFFT}}{\text{FB}} = \frac{2\log_2(N) + 0.8}{\log_2(c) + \log_2(N) + 0.4I + 0.2} \tag{6}$$

Assuming $I = 4$, and $c = 1$, so that both OFFT and the FB use equal length transforms, then in the limit of large N OFFT has twice the complexity. With reasonable length FFTs ($N = 256$) the ratio becomes 1.7. With $I = 4$, equal complexity is established for $c = 128$ which corresponds to a FB whose length is almost the square of the corresponding OFFT. As shown in the next section, the greater frequency resolution provided by the FB results in similar performance to OFFT using shorter FFTs.

2.4.1 Simulation Model

Figure 6 shows the simulation model. All signals are modeled by their complex baseband equivalents. Many details that have little effect on the relative performance of the anti-interference processing techniques, such as down/up frequency conversion, quantization noise, nonlinearities, etc., are ignored. Performance focuses on the time-of-arrival error (which is proportional to pseudorange error) for a single satellite measurement.

The receiver input $r(t)$ comprises three components: the GPS signal $s(t)$, the additive white noise $n(t)$ and the narrowband interference $i(t)$, viz:

$$r(t) = s(t) + n(t) + i(t). \tag{7}$$

As shown in the figure, the sum of these three components is processed by an anti-aliasing filter, sampled, and then processed to remove interference. A time-of-arrival estimate is then extracted using the appropriate sampled reference signal (as filtered by the same anti-aliasing filter).

Figure 6. Simulation Methodology for Examining Anti-Interference Processing Performance

The GPS signal $s(t)$ models the P-code signal used for time-of-arrival estimation. The signal is modeled as BPSK, viz.:

$$s(t) = \sqrt{P_s} \sum_{n=-\infty}^{\infty} a_n p(t - nT) \tag{8}$$

where P_s is the signal power, the coefficients $\{a_n\}$ are simply a pseudorandom sequence of ± 1, $T = 1/10.23$ MHz, and

$$p(t) = \begin{cases} \dfrac{1}{\sqrt{T}}, & |t| < \dfrac{T}{2} \\ 0, & \text{otherwise} \end{cases} . \tag{9}$$

The white noise $n(t)$ is modeled as Gaussian-distributed with power spectral density N_0. The interference is modeled as the sum of M complex sinusoids of the form:

$$i(t) = \sum_{k=1}^{M} A_k e^{2\pi i(f_k t + \phi_k)} \tag{10}$$

where A_k, f_k and ϕ_k are the amplitude, frequency and phase of the k^{th} sinusoid, respectively. The frequencies f_k are selected to be uniformly distributed over $\left(-1/(2T_s), 1/(2T_s)\right)$, where T_s is the sample time and the phases ϕ_k are selected to be uniformly distributed over $(0, 2\pi)$.

The input signal $r(t)$ is assumed to be filtered by an analog anti-aliasing filter, modeled as a lowpass 5th order Butterworth with 3 dB bandwidth of 75% of the sampling frequency. After analog-to-digital conversion the samples are processed by one of the three interference processors discussed in the previous section and then correlated against a sampled version of the reference signal $s(t)$ that has been filtered by the same anti-aliasing filter. This correlation establishes time-of-arrival to within a sample and corrects for any time offsets generated by the interference processing. Improved time-of-arrival resolution is then obtained by correlating against an interpolated version of this reference and then least-square fitting the absolute value of the correlation to a parabola. The abscissa of the peak of the parabola is the estimated signal time-of-arrival.

The time-of-arrival estimated above reflects that obtained from noncoherent peak-picking processing. An actual GPS receiver would more likely use an early-late gate type discriminator that effectively averages over a longer time to achieve a single time-of-arrival estimate. While the discriminator processing modeled here does not reflect certain real-world complications (i.e., response to Doppler shifts) it allows the relative performance of various processing techniques to be assessed efficiently. That is, while the absolute performance in terms of required input SNR for a particular time-of-arrival error may be

shifted from its actual value, the relative performance of competing techniques should be estimated reasonably accurately. Note also that the model is not designed to estimate time-of-arrival for shifts greater than one-half sample from the initially observed peak in the cross correlation function. Again, this is a small limitation since time-of-arrival errors of that magnitude are of little interest.

Section 3

Results

This section describes simulation results aimed at comparing the effect of anti-interference processing on GPS performance. The evaluation focuses on GPS receiver tracking performance, estimated by examining the pseudorange error achieved by a single correlator at various input SNR.

3.1 Simulation Values

The following values are used for initial simulation results. The sample time T_s is set at 40 ns (i.e., 25 MHz bandwidth). Each correlation is over 3072 samples, yielding a processing gain of 35 dB. The interferer frequency and phase is shifted every 160 time-of-arrival estimates, allowing transient effects for the OFFT and the FB to be discarded. (The OFFT approach exhibits a transient in the first FFT after the interference changes, while the filter bank requires *I* FFTs to achieve steady-state performance). The convergence properties of the ATF are also ignored in this analysis. The interference power is normalized such that its total is either 40 dB or 60 dB above the input white noise power.

Based on the earlier complexity discussion the ATF and the FFT technique are assumed to use 35 taps and 256 points, respectively, which have approximately equal complexity (ignoring the relatively small complexity contribution of the threshold algorithm to the OFFT technique). The FB technique uses a $128 \times 4 = 512$ sample filter with a 128-point FFT.

Figure 7 shows the evolving power spectrum estimate of the filter bank for the first 10 blocks of samples. As the effective filter length for this filter bank uses 4 FFTs, it requires approximately 4 blocks to achieve steady-state performance. While not shown, the equivalent FFT-based suppression achieves steady-state response within a single FFT length. From another perspective, its effective filter length is the FFT length.

Figure 8 shows the effect of correcting for the anti-aliasing filter in the coefficient computation for the ATF. The uncorrected (dashed) line shows that the filter attempts to

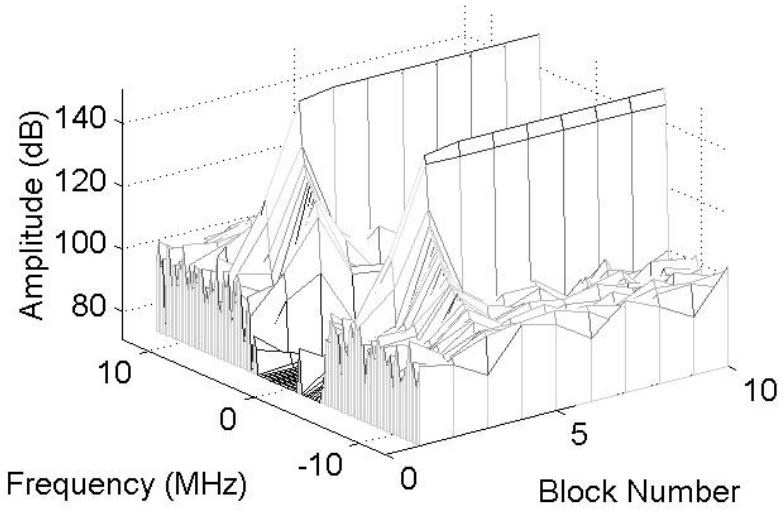

Figure 7. Successive Power Spectra Out of Filter Bank with Two Interferers

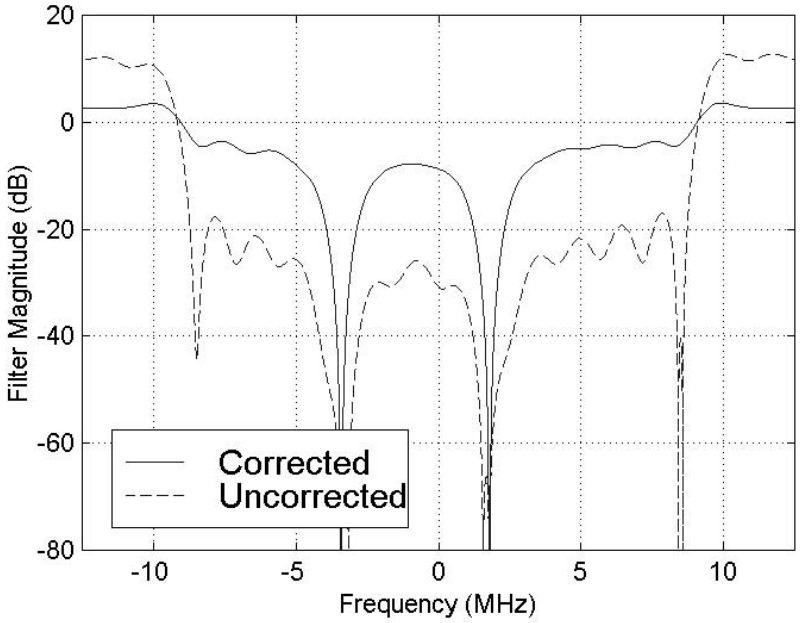

Figure 8. Adaptive Transversal Filter Response Against Two Interferers Both With and Without Correction for Anti-Aliasing Filter

whiten the anti-aliasing filter, wasting coefficients on a spectral region that can be ignored, and generating large amplitude fluctuations in the remaining parts of the spectrum. In contrast, the ATF designed to ignore this anti-aliasing filter shows improved response in terms of both sharper nulls at the interference frequencies and a flatter response away from these frequencies. In the following results the ATF corrects for the effects of the anti-aliasing filter by adding white Gaussian-distributed noise with power equal to that at the receiver front end prior to anti-aliasing filtering. This noise is added only for the coefficient calculation; the actual data samples for ATF processing remain unchanged. While this lowers the SNR for the coefficient calculation, it should have little effect on this calculation since the interference-to-noise power ratio is large.

Figure 9 shows performance without added interference for the three systems and for an ideal system that lacks interference processing**.** Without interference only the ATF is able to match the performance of the ideal system in terms of the input SNR required to achieve a particular time-of-arrival error**.** In this situation the ATF impulse response approximates a

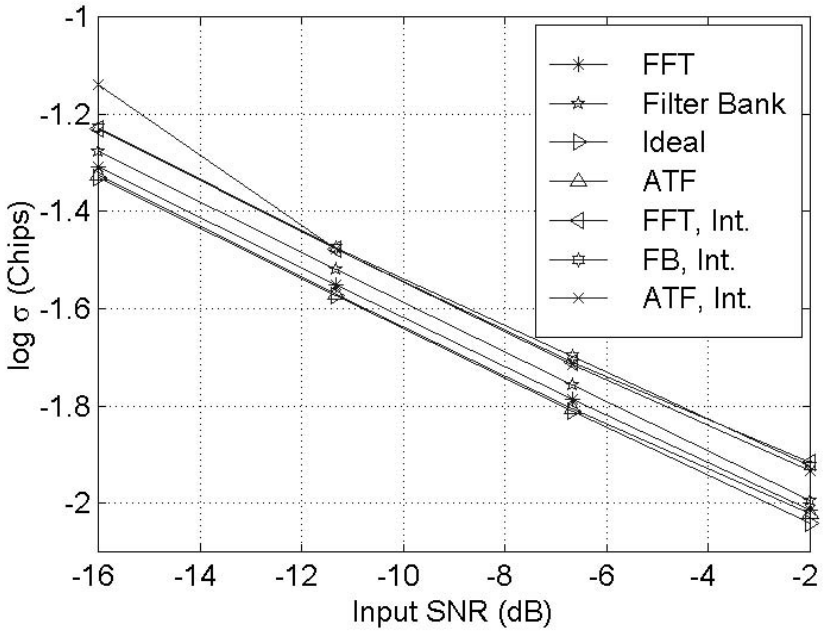

Figure 9. Time-of-Arrival Performance for the 3 Systems With and Without Ten Narrowband Interferers 40 dB Above the Additive Noise

delta function and so causes no insertion loss. The OFFT system and FB system show insertion losses of 0.5 and 1.2 dB, respectively. For the OFFT system this loss closely matches the predicted weighting loss of 0.6 dB, while for the FB system this loss reflects the interference between adjacent filters that prevents perfect reconstruction.

Figure 9 also shows time-of-arrival performance against 10 interferers with their total power 40 dB above the input noise power. While not shown, the ideal system using no interference processing exhibits substantially degraded performance in this environment. The remaining three systems show much less, but non-vanishing degradation when interference is added. Over the higher input SNR range all three systems perform equivalently. The ATF and the OFFT both suffer a 2 dB insertion loss with interference present, while the FB system suffers a 2.4 dB insertion loss with interference. All the systems are removing the interference essentially equally; the FB performs slightly worse because its initial insertion loss without interference is higher.

Each CW interferer is observed to occupy approximately 7 bins for the OFFT and 3 bins for the FB. Ten interferers represent $70/256 = 27\%$ of the band excised for the OFFT and $30/128 = 23\%$ of the band excised for the FB. The number of bins excised per interferer remains approximately constant even as the FFT length increases (for either the OFFT technique or the FB). Consequently, the fraction of the band excised decreases as this length increases. Beyond a certain point (around 10%) however, there is little additional performance benefit of increasing the FFT length. At the lowest input SNR the ATF's performance is slightly inferior to that of the other systems. Additional simulation results (not shown) indicate that with fewer interferers at 40 dB total power relative to the additive white noise the insertion loss of all three techniques against interference gradually approaches that without interference.

Figure 10 shows performance against two interferers with total power 60 dB above the input white noise power. The insertion loss with interference is 0.9 dB for the OFFT and 1.2 dB for the FB. Again, both techniques suffer about the same performance loss from excision; the FB performs slightly worse than the FFT because of its signal reconstruction errors. The ATF's performance with this more powerful interference is substantially

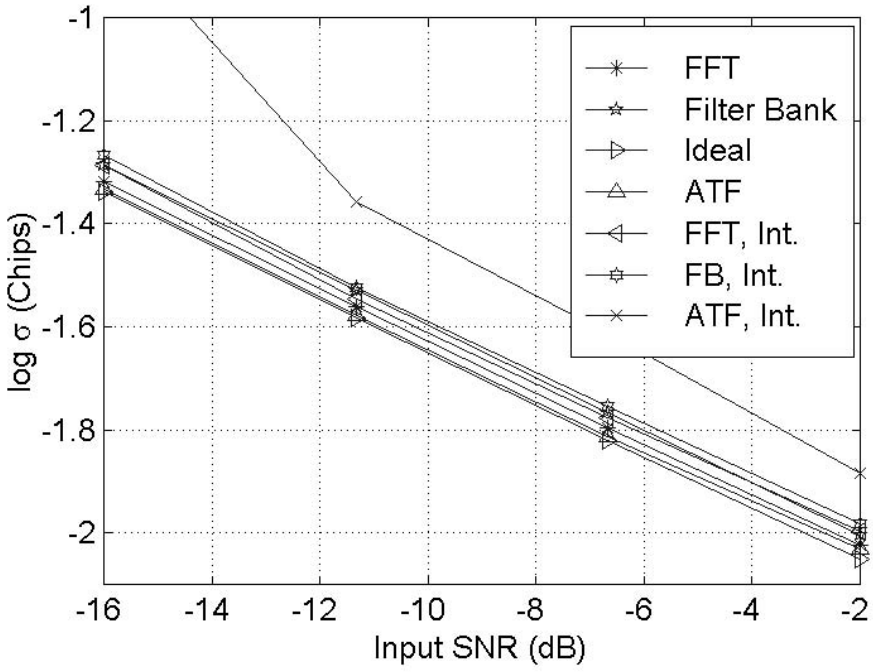

Figure 10. Time-of-Arrival Performance for the 3 Systems With and Without Two Narrowband Interferers 60 dB Above the Additive Noise

degraded, incurring an insertion loss of 3.4 dB with interference. Examination of the ATF frequency response shows that this degradation is caused by large amplitude fluctuations in its frequency response with this more powerful interference. That is, although the interferer is effectively removed by the ATF, the remaining GPS signal spectrum is severely distorted. Consequently, performance suffers. This effect is exacerbated substantially if the ATF is not corrected for its anti-aliasing filter. The previous results in Figure 9 show that for modest interference power all techniques perform reasonably well even with a relatively large number of interferers. The results of Figure 10 show that with higher interference power, even relatively few interferers degrade ATF performance relative to both the OFFT and FB techniques.

With 10 interferers at 60 dB (not shown) these insertion losses increase. For the FB and the OFFT techniques they increase to 2 dB and 2.5 dB, respectively, while for the ATF they increase to 6 dB. For the ATF, additional high-power interferers further degrade the GPS signal spectrum.

Additional analyses (not shown) have been performed with varying numbers of frequency bins. When the FB FFT length is increased from 128 to 256 with 10 interferers a total of 60 dB above the white noise power the insertion loss decreases to 1.5 dB — a 0.2 dB decrease. The performance improvement is modest because the fraction of the band excised with 10 interferers decreases from 23% to 12%, which is too small to make a substantial performance improvement. Thus, for 10 or fewer interferers there is little reason to use more than 128 frequency cells in the FB. Conversely, there is a substantial performance loss when the FFT length decreases from 256 to 128 for the OFFT technique with 10 interferers. Here, the fraction of band excised increases from 27% to 55%, which causes the insertion loss with interference to increase to 10 dB. Table 1 summarizes these results for complexity versus performance with both 2 and 10 interferers 60 dB above the additive white noise.

Table 1. Insertion Losses With and Without 60 dB Interference

	Frequency Cells/Taps	Relative Complexity	Insertion Loss (dB) – No Int.	Insertion Loss (dB) – 2 Int.	Insertion Loss (dB) – 10 Int.
FFT	128	1.7	0.6	2.1	10.0
FFT	256	1.9	0.5	0.9	2.5
ATF	35	1.9	0	3.4	6.0
FB	128	1.0	1.2	1.4	2.0
FB	256	1.1	1.0	1.0	1.5

Section 4

Summary and Conclusions

This paper has examined the performance of three techniques useful for suppressing narrowband interference in GPS. All the techniques filter the interference, leaving the remaining GPS signal slightly degraded. The OFFT technique inherently has the fastest response time, which approximately equals the FFT duration. It would therefore be the most applicable technique in a changing interference environment. FM chirp-type interference represents one such environment. The FB technique has the lowest complexity for a given level of performance. Its response time depends on its design and is typically twice as long as that of the OFFT technique. The ATF has the lowest interference-free insertion loss within this group, but typically has the longest response time. Both the OFFT and the FB require a separate threshold algorithm; the ATF inherently uses no threshold. The ATF requires some form of data pre-processing to assure that the anti-aliasing filter that precedes analog-to-digital conversion does not affect its coefficient calculation. Without such pre-processing the ATF's performance is substantially degraded.

Performance was quantified in terms of the increase in required input SNR to achieve a particular time-of-arrival error, as compared to that for an ideal system operating in white Gaussian-distributed noise. Convergence effects for both the ATF and the FB were ignored. Additionally, the performance comparisons focused specifically on pseudorange error for GPS; acquisition performance was ignored. It is expected, however, that acquisition performance would be similarly affected by the interference processing.

Additional results established approximate rules of thumb for deciding on the number of required frequency cells for either the FB or the OFFT technique against several narrowband interferers. With the weighting techniques adopted here each interferer occupies approximately 3 (7) bins for the FB (OFFT) technique. So long as the fraction of the band excised remains below approximately 25% there is little performance degradation. However,

when this fraction approaches 50% the insertion loss increases several dBs. Thus, a 256-bin OFFT can handle approximately $0.25*256/7 \approx 9$ interferers while a 128-frequency cell FB can handle approximately $0.25*128/3 \approx 11$ interferers.

List of References

1. DiFranco, J. V. and W. L. Rubin, "Radar Detection," Artech House, Dedham, Massachusetts, (1981).

2. Kolodziejski, K. R., and J. W. Betz, "Effect of Non-White Gaussian Interference on GPS Code Tracking Accuracy," MITRE MTR 99B0000021R1, The MITRE Corporation, Bedford, Massachusetts, (June 1999).

3. Milstein, L. B., "Interference Rejection Techniques in Spread Spectrum Communications," *Proc. IEEE*, Vol. 76, No. 6, June 1988.

4. Capozza, P. T., B. J. Holland, T. M. Hopkinson, R. L. Landrau, "A Single-Chip Narrowband Frequency Domain Excisor for a Global Positioning System (GPS) Receiver, " Custom Integrated Circuits Conference, May 16-19, San Diego, California.

5. Crochiere, R. E. and L. R. Rabiner, "Multirate Digital Signal Processing," Prentice-Hall, Inc., Englewood Cliffs, New Jersey, (1983).

6. Jones, W. W., and K. R. Jones, "Narrowband Interference Suppression Using Filter-Bank Analysis/Synthesis Techniques," IEEE MILCOM Conference, San Diego, California, Paper 38.1.1, (1992).

7. Haykin, S., "Adaptive Filter Theory," Prentice Hall, Englewood Cliffs, New Jersey, (1986).